Organic Electronics 59 (2018) 220–223

Contents lists available at ScienceDirect

Organic Electronics

journal homepage: www.elsevier.com/locate/orgel

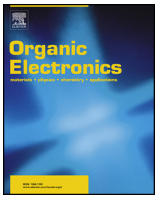

Silver-induced activation of 8-hydroxyquinolinato lithium as electron injection material in single-stack and tandem OLED devices

Felipe A. Angel[a,b,*], Rui Gao[b], Jason U. Wallace[c], Ching W. Tang[b,d]

[a] Departamento de Química Inorgánica, Facultad de Química, Pontificia Universidad Católica de Chile, Santiago 7820436, Chile
[b] Department of Chemical Engineering, University of Rochester, Rochester, NY 14627, USA
[c] Department of Chemistry, D'Youville College, Buffalo, NY 14201, USA
[d] Institute for Advanced Study, Hong Kong University of Science and Technology, Clear Water Bay, Kowloon, HK, China

ARTICLE INFO

Keywords:
Lithium quinolate
OLED
Tandem structure
Charge-generation layer

ABSTRACT

The 8-hydroxyquinolinato lithium (Liq)|Ag system has been evaluated as the electron-injection layer for the MoO_x| N,N′-di (1-naphthyl)-N,N′-diphenyl-(1,1′-biphenyl)-4,4′-diamine (NPB) charge-generation layer in tandem organic light-emitting diode (OLED) devices. From current-voltage studies of single-stack devices, it is determined that Liq is a relatively poor electron-transport material. However, Liq is found to be useful as an electron-injection layer with activation by Ag. Efficient tandem devices have been obtained using Liq|Ag as the electron-injection layer adjacent to the MoO_x|NPB charge-generation layer, where the optimal Ag thickness is about 20–40 Å and the activation of Liq can be seen with as little as 1 Å of Ag.

1. Introduction

Tandem organic light-emitting diode (OLED) devices are useful for display and lighting applications where high brightness is necessary. In a tandem OLED device, two or more individual electroluminescent (EL) cells are physically stacked in parallel and electrically connected in series by a common interconnect layer, also known as charge-generation layer (CGL) [1,2]. An ideal CGL should have minimal electrical impedance and highest optical transparency, in addition to providing ohmic contacts to the adjacent EL cells. Several CGL compositions have been reported, typically formed by n-type|p-type or transition metal oxide|p-type interface [3–7]. A commonly used transition metal oxide material is MoO_x, which is relatively stable and readily vapor-deposited as a thin film from an air-stable MoO_3 source. A key aspect to produce efficient tandem devices is the charge injection from the CGL to the adjacent EL cells. For electron injection materials, Li metal with a low work function is useful. However, the handling of Li metal is inconvenient, if not hazardous, for vapor deposition. Alternately, air-stable lithium compounds, such as Li_3N, can be used as a Li deposition source, which release Li metal upon heating [8]. Rather than generating Li metal from an evaporation source, n-type Li-doped contacts can be produced by activating a deposited film of Li-containing compound, such as the archetypical LiF, or molecule, such as 8-hydroxyquinolinato lithium (Liq) [9] and other derivatives [10–12], typically with an overlayer of vapor-deposited Al [13–16]. In this work, we have examined specifically Liq|Ag for application as electron-injection layer (EIL) of the MoO_x|NPB CGL, and will show that Ag, despite its slightly higher work function, is as effective as Al in activating Liq to form an n-doped electron-injecting contact, offering an alternative to Al, a widely used metal in organic electronic devices despite its tendency to alloy with refractory metals, causing unstable deposition rates and reducing the lifetime of the sources, whether is a thermal or e-beam evaporation source.

2. Experimental

OLED devices were fabricated on pre-patterned indium tin oxide (ITO) (~1000 Å) glass substrates (1.5 × 1.5 inches) with a surface resistance of ~15 Ω/sq and an optical transparency of ~90%. The ITO substrates were batch-wise cleaned by scrubbing with detergent solution, then rinsed, and subjected to 10 min agitation in ultrasonic baths of DI water, acetone, and isopropanol, sequentially. Following a final isopropanol rinse, the substrates were dried with nitrogen and treated with oxygen plasma (2:15 min, 400 W and 5×10^{-1} mbar). All films were prepared by vapor deposition in a vacuum chamber ($< 5.0 \times 10^{-6}$ Torr) without breaking vacuum until the OLED device was completed with a 1000 Å top silver electrode, at a constant rate of 5.0 Å/s for silver. A typical layer sequence is as follows: A 20 Å layer of molybdenum oxide (MoO_x) was deposited at about 0.3 Å/s on ITO as the hole-injecting layer (HIL), N,N′-di (1-naphthyl)-N,N′-diphenyl-(1,1′-

---

[*] Corresponding author. Departamento de Química Inorgánica, Facultad de Química, Pontificia Universidad Católica de Chile, Santiago 7820436, Chile.
E-mail address: faangel@uc.cl (F.A. Angel).

https://doi.org/10.1016/j.orgel.2018.05.023
Received 13 April 2018; Received in revised form 10 May 2018; Accepted 15 May 2018

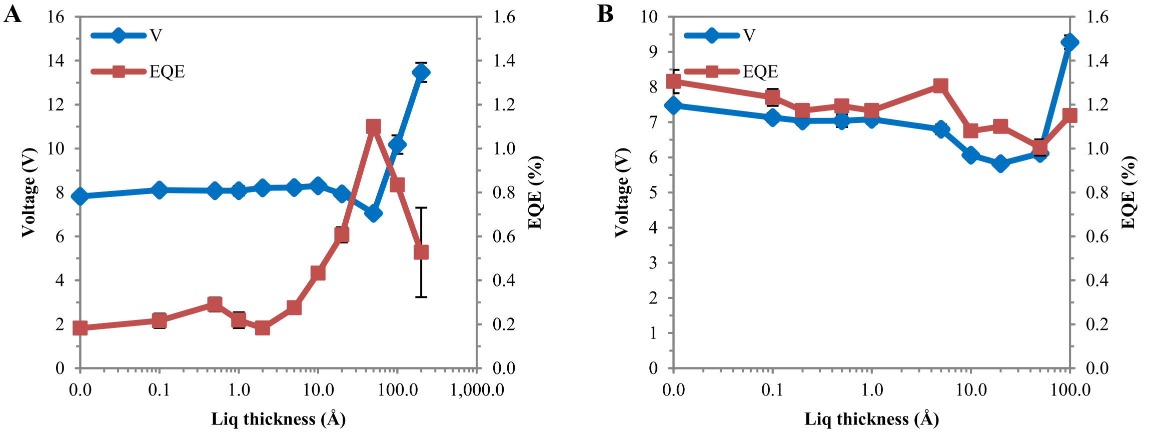

Fig. 1. Drive voltage and EQE dependence on Liq thickness for devices: (A) ITO|MoO$_x$ (20 Å)|NPB(600 Å)|Alq$_3$ (400 Å)|**Liq(x)**|Ag, and (B) ITO|MoO$_x$ (20 Å)|NPB (600 Å)|Alq$_3$ (400 Å)|Bphen (100 Å)|**Liq(x)**|Ag. The voltage and EQE were measured at 20 mA/cm^2.

biphenyl)-4,4′-diamine (NPB) was the hole transport layer (HTL), tris (8-hydroxyquinolinato) aluminum (Alq$_3$) was the electron transport layer (ETL) as well as the light emitter, 4,7-diphenyl-1,10-phenanthroline (Bphen) was the optional ETL, and 8-hydroxyquinolinato lithium (Liq) was the electron-injecting layer (EIL). The deposition rates for the organic layers were typically 4 Å/s. For Liq and silver thickness dependence experiments, 0.1 Å/s and 1.0 Å/s were used for layer thicknesses below and above 1 Å, respectively. Four identical OLED devices with an active area of 0.1 cm^2 were produced on a single substrate. The electroluminescent properties of the devices were recorded with a Photoresearch PR650 SpectraScan Colorimeter and a Keithley 2400 source meter.

3. Results and discussion

3.1. Single-stack devices

We first evaluated Liq as the ETL in a series of single-stack OLED devices (Devices A) – ITO|MoO$_x$ (20 Å)|NPB(600 Å)|Alq$_3$ (400 Å)|**Liq (x)**|Ag – where Liq is adjacent to the Alq$_3$ emitting layer. The Liq thickness was varied from 0 to 200 Å. As shown in Fig. 1A, the external quantum efficiency (EQE) is very low (~0.2%) without the Liq layer, due to apparently the penetration of Ag into Alq$_3$ during Ag deposition. The EQE starts to increase around 2 Å of Liq and reaches a maximum of ~1.1% around 50 Å, while the drive voltage remains relatively constant at ~8 V throughout this thickness range. Beyond 50 Å, the EQE decreases rapidly while the voltage increases sharply, to 0.5% and 13.5 V at 200 Å Liq, respectively. This variation of EQE and drive voltage with the Liq thickness can be attributed to the degree of Ag penetration (with Ag as a quencher) into Alq$_3$. Acting as a buffer layer, Liq impedes the penetration of Ag. It has been previously reported that Ag can diffuse deeply into Alq$_3$ in the absence of a buffer layer, such as Bphen [17–19]. Our data show that Liq is effective as a buffer, but, unlike Bphen, it is not a good ETL. The sharp voltage rise with Liq thickness larger than 50 Å indicates that the interaction between Ag and Liq is limited to 50 Å and that the transport of electrons in a neat Liq layer is relatively poor. The corresponding drop in EQE is likely a result of a shift of the electron-hole recombination zone from the NPB|Alq$_3$ interface towards the Alq$_3$|Liq interface, where the proximity of the Ag electrode causes quenching.

Next, we evaluated Liq as the EIL in another series of single-stack devices (Devices B) – ITO|MoOx (20 Å)|NPB(600 Å)|Alq$_3$ (400 Å)|Bphen (100 Å)|**Liq(x)**|Ag – where a separate ETL, Bphen (100 Å), was inserted between the Alq$_3$ and Liq layers. The thickness of the Liq layer was varied between 0 and 100 Å. As shown in Fig. 1B, the EQE values for Devices B are uniformly high compared to Devices A, varying between 1.3% and 1.0%. Also, the drive voltage is lower compared to Devices A, reaching a minimum of 5.8 V around 20 Å of Liq. These results demonstrate that Ag chemically interacts with Liq during Ag deposition to form an electron-injecting contact. The optimal Liq thickness is about 20 Å.

Liq|Ag electron-injecting contacts where further investigated using two sets of devices: Devices C: ITO|MoO$_x$ (20 Å)|NPB(600 Å)|Alq$_3$ (400 Å)|**Bphen:Liq(100 Å:x%)**|Ag, and Devices D: ITO|MoO$_x$ (20 Å)|NPB(600 Å)|Alq$_3$ (400 Å)|**Bphen:Liq(100 Å:x%)**|Liq (20 Å)|Ag. The difference between these two sets of devices is an additional Liq

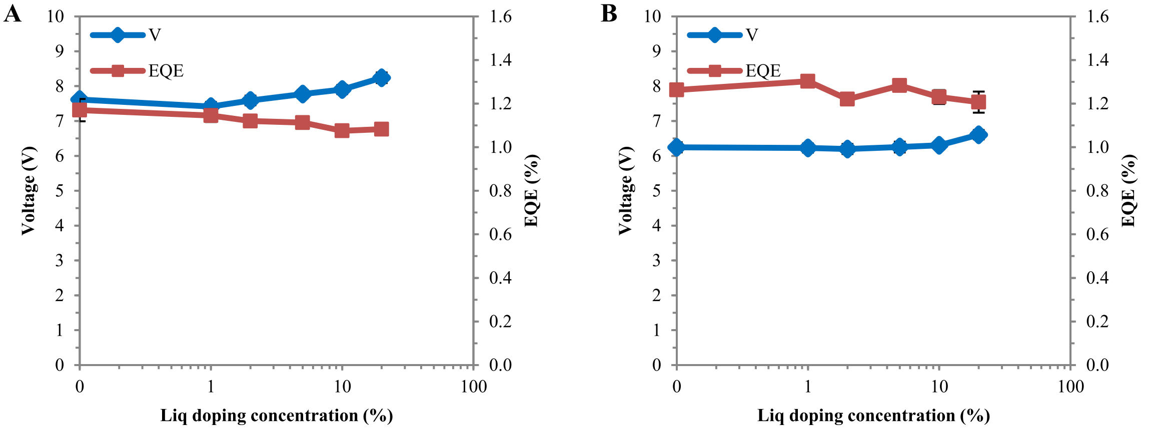

Fig. 2. Drive voltage and EQE dependence on Liq doping concentration for devices: (C) ITO|MoO$_x$ (20 Å)|NPB(600 Å)|Alq$_3$ (400 Å)|**Bphen:Liq(100 Å:x%)**|Ag, and (D) ITO|MoO$_x$ (20 Å)|NPB(600 Å)|Alq$_3$ (400 Å)|**Bphen:Liq(100 Å:x%)**|Liq (20 Å)|Ag. The voltage and EQE were measured at 20 mA/cm^2.

(20 Å) layer in contact with the Ag electrode. As shown in Fig. 2A for Devices C without the Liq (20 Å) layer, the drive voltage increases (from 7.6 V to 8.2 V) and the EQE decreases (from 1.2% to 1.0%), both linearly, as the Liq component in the Bphen:Liq mixture is increased (from 0% to 20%). In contrast, as shown in Fig. 2B, there is less variation in both drive voltage and EQE for Devices D with a Liq (20 Å) layer. Also noteworthy is that the drive voltage for Devices D is lower than Devices C by more than 1 V. These results indicate that doping Liq into Bphen (up to 20%) has relatively little effect on producing electron-injecting contact with Ag. In fact, Liq appears only to reduce the electron mobility in a Bphen:Liq mixture by diluting the Bphen component. Previous reports have shown an improved electron-injecting contact with a Liq-doped Bphen layer [11,20–23]. However, the improvements were obtained with Al instead of Ag as the cathode metal, which is consistent with the fact that Al, being highly reactive, can react with both Liq and Bphen to form the electron-injecting contact. Whereas with a less reactive Ag as the cathode, an efficient electron-injection contact, Liq|Ag, can only be obtained with a neat Liq layer. By contrasting these results to those from Devices A and B, it is clear that Liq|Ag is useful in forming the EIL adjacent to the CGL in tandem devices.

3.2. Tandem devices

Following the characterization of Liq|Ag as the electron-injection contact in the single-stack devices, we proceeded to fabricate tandem devices with Liq|Ag as the as the EIL for the MoO$_x$|NPB CGL. The layer structure with symmetrical front and back units is as follows: ITO|MoO$_x$ (20 Å)|NPB(600 Å)|Alq$_3$ (400 Å)|Bphen (100 Å)|**Liq(20 Å)|Ag (x)**|MoO$_x$ (20 Å)|NPB(600 Å)|Alq$_3$ (400 Å)|Bphen (100 Å)|Liq (20 Å)|Ag. The thickness of Ag in the EIL was varied from 0 to 50 Å. As shown in Fig. 3, functional tandem devices with a drive voltage around 14 V and an EQE of 2.2% have been obtained with Ag of thickness around 10-20 Å. These voltage and EQE values approximately double those of single-stack devices, indicating that Liq|Ag is an effective EIL, even compared to tandem devices with EIL consisting exclusively of Liq (Fig. S1) or Ag (Fig. S2). Further increase in Ag thickness reduces EQE due to light absorption, as expected. It is also interesting to note that a Ag layer as thin as 1 Å can activate electron injection in Liq.

The electrical properties of the EIL were further evaluated by studying the JV characteristics of tandem devices where the charge carriers injected from the electrodes can be decoupled from those generated and injected by the CGL. For this purpose, a set of "single-carrier" devices with the following layer configuration was fabricated: ITO|Alq$_3$ (400 Å)|Bphen (100 Å)|**EIL**|MoO$_x$ (20 Å)|NPB(600 Å) |Ag, where the formulation of the EIL comprised: 1) Liq|Ag and 2) Liq. In this configuration, hole injection from ITO and electron injection from Ag are purposely blocked with Alq$_3$ and NPB as the respective hole-transport and electron-transport layers. Consequently, the JV characteristics should reflect only the efficiency of charge generation and the injection of holes (into NPB), and electrons (into Bphen) from the EIL. As shown in Fig. 4, JV characteristics are highly dependent on the nature of the EIL. With a fully functional EIL, Liq (40 Å)|Ag (40 Å), which is similar to the one used in the tandem devices of Fig. 3, the JV is normal, indicating efficient injection of electrons, from Liq|Ag to Bphen. With a neat layer of Liq (40 Å) as EIL, there is a very large voltage shift (~15 V) in the JV characteristics, indicating poor electron injection efficiency from unactivated Liq. It should be noted that similar inefficiency is observed in the tandem cells of Fig. 3 with neat Liq as the EIL.

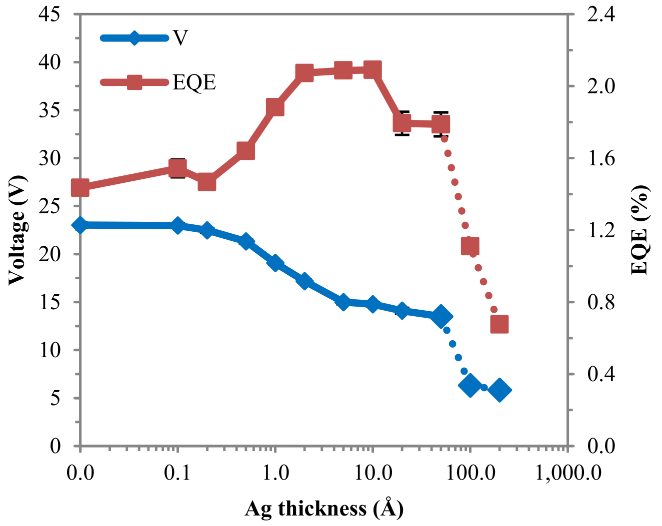

Fig. 3. Drive voltage and EQE dependence on Liq thickness for: ITO|MoO$_x$ (20 Å)|NPB(600 Å)|Alq$_3$ (400 Å)|Bphen (100 Å)|Liq (20 Å)|**Ag(x)**|MoO$_x$ (20 Å)|NPB(600 Å)|Alq$_3$ (400 Å)|Bphen (100 Å)|Liq (20 Å)|Ag devices. The voltage and EQE were measured at 20 mA/cm^2.

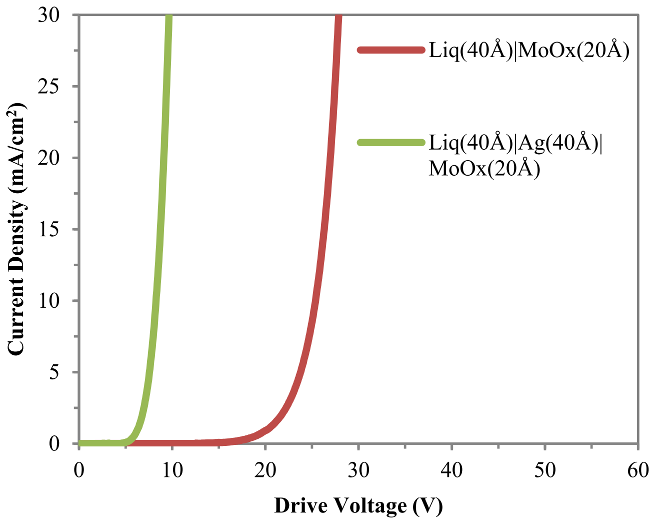

Fig. 4. Current density-voltage characteristics for: ITO|Alq$_3$ (400 Å)|Bphen (100 Å)|**EIL**|MoO$_x$ (20 Å)|NPB(600 Å)|Ag devices, where the EIL is 1) Liq (40 Å)|Ag (40 Å) and 2) Liq (40 Å).

Most reports rather use Al as the metal cathode with Liq as the EIL [13–15], despite the intrinsic difficulties related to Al deposition through thermal and e-beam evaporation. Comparing Al and Ag, both metals have similar sublimation temperature, work function, and atomic size. Liu et al. justified the slightly lower device performance observed with Ag due to its low reactivity, compared to Ca, Mg, and Al [24]. We compared Ag, Cu, and Al for use as the cathode metal in the EIL. As shown in Fig. 5, the JV characteristics for the two-stack tandem devices, ITO|MoO$_x$ (20 Å)|NPB(600 Å)|Alq$_3$ (400 Å)|Bphen (100 Å)|Liq (40 Å)|**Metal(40 Å)**|MoO$_x$ (20 Å)|NPB(600 Å)|Alq$_3$ (400 Å)|Bphen (100 Å)|Liq (20 Å)|Ag, are highly dependent on the composition of the CGL. With Ag and Al as the cathode, the tandem devices behave normally requiring a drive voltage of 12.7 V and 12.9 V, respectively, which is double that of the corresponding single-stack devices. Cu produced an inferior tandem device with a distinctly higher drive voltage of 17 V. The EQE values revealed a similar trend with a value of about 2% for Ag and Al and a lower value of 1.7% for Cu. This dependence of the device performance on the metal electrode may be attributed to the difference in their work functions, and the resulting energy barrier between the n-doped electron-injecting layer and MoO$_x$ work function [6,7]. With a higher work function, Cu (~4.7eV) is less reactive and not as effective as either Al or Ag (both ~4.3eV) activating Liq and forming the necessary electron-injecting contact between EL cells. This is consistent with Liu et al. [24], and recent results from Shi et al. [5], where Liq was effectively activated even with a low work

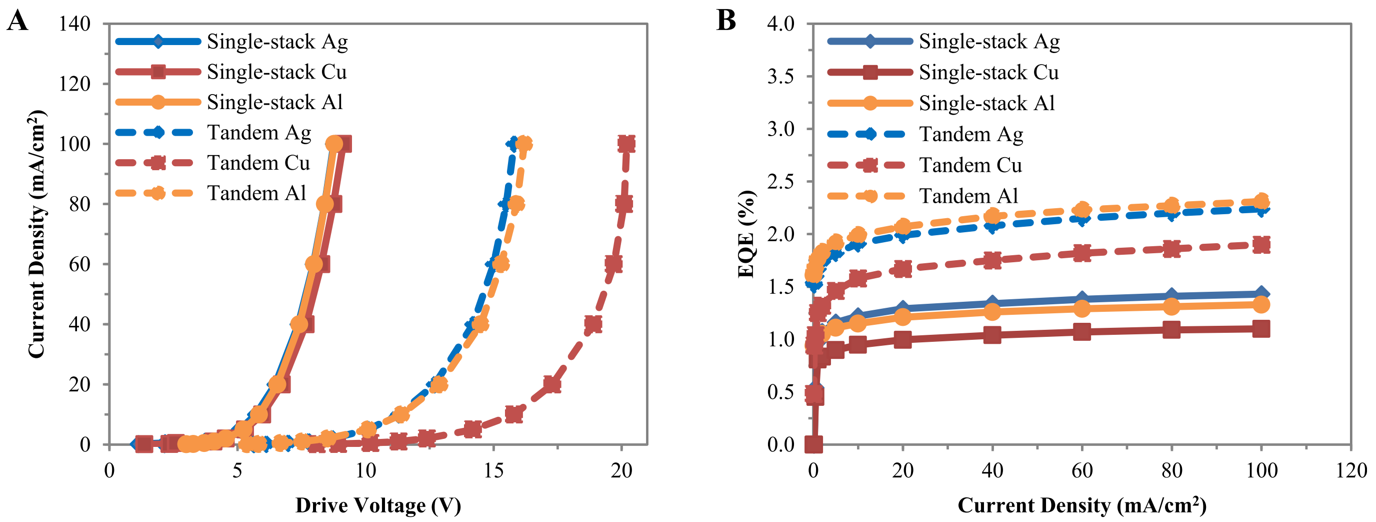

Fig. 5. Current density-voltage (A) and current density-external quantum efficiency (B) characteristics for two-stack tandem devices: ITO|MoO$_x$ (20 Å)|NPB (600 Å)|Alq$_3$ (400 Å)|Bphen (100 Å)|Liq (40 Å)|**Metal(40 Å)**|MoO$_x$ (20 Å)|NPB(600 Å)|Alq$_3$ (400 Å)|Bphen (100 Å)|Liq (20 Å)|Ag.

function metal such as Ca in tandem devices. Our results further support that low work function and more compatible metals with thermal evaporation can produce efficient tandem devices, with Liq as n-doped electron-injecting layer.

4. Conclusions

We have evaluated Liq|Ag for applications as the electron-injection layer in tandem OLED devices. Using single-stack devices, Liq, as a neat material, was found to be a relatively poor electron-transport layer compared to other common electron-transport materials such as Bphen. However, Liq was found to be effective as an electron-injection layer up to a thickness of about 40 Å with an overlayer of vapor-deposited Ag. We have obtained efficient tandem devices using Liq|Ag as the electron-injection layer, where the optimal Ag thickness is about 20–40 Å and the activation of Liq can be affected with as little as 1 Å of Ag.

Acknowledgment

This work was supported by eMagin Corporation.

Appendix A. Supplementary data

Supplementary data related to this article can be found at http://dx.doi.org/10.1016/j.orgel.2018.05.023.

References

[1] M.-K. Fung, Y.-Q. Li, L.-S. Liao, Tandem organic light-emitting diodes, Adv. Mater. 28 (2016) 10381.
[2] T. Chiba, Y.-J. Pu, J. Kido, Organic light-emitting devices with tandem structure, Top. Curr. Chem. 374 (2016) 33.
[3] J.H. Jou, S. Kumar, A. Agrawal, T.H. Li, S. Sahoo, Approaches for fabricating high efficiency organic light emitting diodes, J. Mater. Chem. C 3 (2015) 2974.
[4] H.D. Sun, Q.X. Guo, D.Z. Yang, Y.H. Chen, J.S. Chen, D.G. Ma, High efficiency tandem organic light emitting diode using an organic heterojunction as the charge generation layer: an investigation into the charge generation model and device performance, ACS Photonics 2 (2015) 271.
[5] C. Shi, N. Sun, Z. Wu, J. Chen, D. Ma, High performance hybrid tandem white organic light-emitting diodes by using a novel intermediate connector, J. Mater. Chem. C 6 (2018) 767.
[6] K. Hong, J.-L. Lee, Charge generation mechanism of metal oxide interconnection in tandem organic light emitting diodes, J. Phys. Chem. C 116 (2012) 6427.
[7] S. Hamwi, J. Meyer, M. Kröger, T. Winkler, M. Witte, T. Riedl, A. Kahn, W. Kowalsky, The role of transition metal oxides in charge-generation layers for stacked organic light-emitting diodes, Adv. Funct. Mater. 20 (2010) 1762.
[8] L. Duan, Q. Liu, Y. Li, Y. Gao, G. Zhang, D. Zhang, L. Wang, Y. Qiu, Thermally decomposable lithium nitride as an electron injection material for highly efficient and stable OLEDs, J. Phys. Chem. C 113 (2009) 13386.
[9] C. Schmitz, H.W. Schmidt, M. Thelakkat, Lithium-quinolate complexes as emitter and interface materials in organic light-emitting diodes, Chem. Mater. 12 (2000) 3012.
[10] Y.-J. Pu, M. Miyamoto, K.-i. Nakayama, T. Oyama, Y. Masaaki, J. Kido, Lithium phenolate complexes for an electron injection layer in organic light-emitting diodes, Org. Electron. 10 (2009) 228.
[11] E. Jun, M. Toshio, K. Junji, Organic electroluminescent devices having metal complexes as cathode interface layer, Jpn. J. Appl. Phys. 41 (2002) L800.
[12] L.S. Sapochak, F.L. Endrino, J.B. Marshall, D.P. Fogarty, N.M. Washton, S. Nanayakkara, Ligand Methylation and Coordination Geometry Effects on the Properties of Zinc and Lithium (8-Quinolinolato) Chelate Electroluminescent Materials, Molecules as Components of Electronic Devices, American Chemical Society, 2003 p. 171.
[13] Y. Dai, H. Zhang, Z. Zhang, Y. Liu, J. Chen, D. Ma, Highly efficient and stable tandem organic light-emitting devices based on HAT-CN/HAT-CN: TAPC/TAPC as a charge generation layer, J. Mater. Chem. C 3 (2015) 6809.
[14] J. Liu, S. Huang, X. Shi, X. Wu, J. Wang, G. He, Charge separation process in an ultrathin electron-injecting bilayer-assisted charge generation unit for tandem organic light-emitting diodes, J. Phys. Chem. C 117 (2013) 13887.
[15] H. Sasabe, K. Minamoto, Y.-J. Pu, M. Hirasawa, J. Kido, Ultra high-efficiency multi-photon emission blue phosphorescent OLEDs with external quantum efficiency exceeding 40%, Org. Electron. 13 (2012) 2615.
[16] J.H. Kwon, J.Y. Lee, High efficiency and long lifetime in organic light-emitting diodes using bilayer electron injection structure, Synth. Met. 159 (2009) 1292.
[17] S. Fladischer, A. Neuhold, E. Kraker, T. Haber, B. Lamprecht, I. Salzmann, R. Resel, W. Grogger, Diffusion of Ag into organic semiconducting materials: a combined analytical study using transmission electron microscopy and x-ray reflectivity, ACS Appl. Mater. Interfaces 4 (2012) 5608.
[18] H. Yoshida, Electron transport in bathocuproine inter layer in organic semiconductor devices, J. Phys. Chem. C 119 (2015) 24459.
[19] F.A. Angel, J.U. Wallace, C.W. Tang, Effect of lithium and silver diffusion in single-stack and tandem OLED devices, Org. Electron. 42 (2017) 102.
[20] B.Y. Kim, S.J. Lee, J.R. Koo, S.E. Lee, K.H. Lee, J.A. Yoon, W.Y. Kim, S.S. Yoon, Y.K. Kim, Efficient green phosphorescent organic light-emitting diodes depending on concentration of lithium quinolate in electron transport layer, J. Nanosci. Nanotechnol. 13 (2013) 7998.
[21] H.M. Kim, J.H. Seo, W.K. Han, K.H. Lee, H.J. Kang, S.S. Yoon, Y.K. Kim, Improvement of mixed electron transport structure red phosphorescent organic light-emitting diodes, Mol. Cryst. Liq. Cryst. 538 (2011) 53.
[22] C. Sung Hoon, L. Seok Jong, L. Kwang Yeon, Y. Hee Seok, H. Kyu-il, K. Kwang Hyun, K. Sang Dae, B. Hyo Dae, T. Yoon Heung, Improved efficiency and lifetime of organic light-emitting diode with lithium-quinolate-doped electron transport layer, Jpn. J. Appl. Phys. 48 (2009) 062101.
[23] J. Wang, X. Shi, J. Liu, S. Huang, X. Wu, Z. Ye, J. Lu, Y. Su, G. He, P.110: high-efficiency OLEDs based on the gradient doping in transporting layers, SID Int. - Symp. Dig. Tech. Pap. 44 (2013) 1400.
[24] Z. Liu, O.V. Salata, N. Male, Improved electron injection in organic LED with lithium quinolate/aluminium cathode, Synth. Met. 128 (2002) 211.